Published in final edited form as:
Brain Res. 2008 September 16; 1230: 247–257. doi:10.1016/j.brainres.2008.06.127.

Histological and functional outcomes after traumatic brain injury in mice null for the erythropoietin receptor in the central nervous system

Ye Xiong[a], **Asim Mahmood**[a], **Dunyue Lu**[c], **Changsheng Qu**[a], **Humaira Kazmi**[a], **Anton Goussev**[a], **Zhenggang Zhang**[b], **Constance T. Noguchi**[d], **Timothy Schallert**[e], and **Michael Chopp**[b,f,*]

a*Department of Neurosurgery, Henry Ford Health System, 2799 W Grand Blvd, Detroit, MI, 48202, USA*

b*Department of Neurology, Henry Ford Health System, 2799 W Grand Blvd, Detroit, MI, 48202, USA*

c*Department of Psychiatry, State University of New York at Downstate Medical Center, 450 Clarkson Ave, Brooklyn, NY 11203, USA*

d*Molecular Medicine Branch, NIDDK, National Institutes of Health, Bethesda, Maryland 20892, USA*

e*Department of Psychology and Institute for Neuroscience, University of Texas at Austin, Austin, Texas 78712, USA*

f*Department of Physics, Oakland University, Rochester, MI 48309, USA*

Abstract

Erythropoietin (EPO) and its receptor (EPOR), essential for erythropoiesis, are expressed in the nervous system. Recombinant human EPO treatment promotes functional outcome after traumatic brain injury (TBI) and stroke, suggesting that the endogenous EPO/EPOR system plays an important role in neuroprotection and neurorestoration. This study was designed to investigate effects of the EPOR on histological and functional outcomes after TBI. Experimental TBI was induced in adult EPOR-null and wild-type mice by controlled cortical impact. Neurological function was assessed using the modified Morris Water Maze and footfault tests. Animals were sacrificed 35 days after injury and brain sections stained for immunohistochemistry. As compared to the wild-type injured mice, EPOR-null mice did not exhibit higher susceptibility to TBI as exemplified by tissue loss in the cortex, cell loss in the dentate gyrus, impaired spatial learning, angiogenesis and cell proliferation. We observed that less cortical neurogenesis occurred and that sensorimotor function (i.e., footfault) was more impaired in the EPOR-null mice after TBI. Co-accumulation of amyloid precursor protein (axonal injury marker) and calcium was observed in the ipsilateral thalamus in both EPOR-null and wild-type mice after TBI with more calcium deposits present in the wild-type mice. This study demonstrates for the first time that EPOR null in the nervous system aggravates sensorimotor deficits, impairs cortical neurogenesis and reduces thalamic calcium precipitation after TBI.

* Address correspondence and reprint requests to: Michael Chopp, Ph.D., Department of Neurology, Henry Ford Health System, 2799 West Grand Boulevard, Detroit, MI 48202, Tel: 313-916-3936, Fax: 313-916-1318, Email: chopp@neuro.hfh.edu.

Keywords

cell proliferation; erythropoietin receptor null; mouse; sensorimotor; spatial learning; traumatic brain injury

1. Introduction

Erythropoietin (EPO) and its receptor (EPOR), essential for erythropoiesis, are also expressed in the nervous system. EPO treatment promotes functional outcome and enhances neurogenesis after TBI in rats (Lu et al., 2005) and mice (Xiong et al., 2007). EPO also improves neurological outcome in animal models of stroke (Wang et al., 2004) and autoimmune encephalomyelitis (Zhang et al., 2005). EPO promotes neuroprotection; it lowers the blood-brain barrier breakdown (Grasso et al., 2007), and reduces edema (Verdonck et al., 2007) and lesion volume (Brines et al., 2000; Cherian et al., 2007) after TBI. Inhibition of EPO activity by the administration of soluble EPOR worsens the severity of neuronal injury (Sakanaka et al., 1998), suggesting that endogenous EPO is directly involved in an intrinsic neuronal repair pathway. Collectively, these findings indicate that the EPO/EPOR system plays an important role in neuroprotection and neurorestoration.

It has been reported that EPOR-null mice rescued with selective EPOR expression driven by the endogenous EPOR promoter in hematopoietic tissue but not in the brain exhibit normal hematopoiesis and erythropoiesis and survive to adulthood (Chen et al., 2007). Neural cell apoptosis increases in embryonic brain, and neural cell proliferation decreases in the neurogenic zones of adult EPOR-null mice (Chen et al., 2007; Tsai et al., 2006). Neural cells from EPOR-null mice are more sensitive to hypoxia and glutamate toxicity than normal neurons (Chen et al., 2007). These observations demonstrate that endogenous EPO/EPOR signaling plays a critical role in embryonic neural cell survival and neural cell proliferation in adult brain regions associated with neurogenesis. However, it is not known whether EPOR null in the nervous system affects histological and functional outcomes in mice after TBI.

A controlled cortical impact (CCI) model is one of the most widely used TBI models in animals (Fox and Faden, 1998; Hall et al., 2008; Smith et al., 1995; Xiong et al., 2005). Accordingly, using a CCI-induced TBI mouse model, we investigated the effects of EPOR null in the nervous system on cortical and hippocampal injury, cell proliferation, neurogenesis, angiogenesis, axonal injury, sensorimotor function and spatial learning performance.

2. Results

2.1 Lesion volume

Mice were sacrificed at 35 days post TBI for lesion volume measurements. TBI caused a similar volume of tissue loss (about 8%) in the ipsilateral hemisphere compared with the contralateral hemisphere in both wild-type and EPOR-null mice.

2.2 Cell loss in the dentate gyrus (DG)

When examined at 35 days post TBI, the neuron counts in the ipsilateral DG had decreased to 64% of the number found in the DG of corresponding sham animals (Fig. 1, $P<0.05$). No significant difference was observed in the neuron numbers between wild-type and EPOR-null mice after TBI.

2.3 Spatial learning performance

In the present study the modified Morris water maze (MWM) protocol was used to detect spatial learning deficits. As shown in Fig. 2, the time spent in the correct quadrant (Northeast) by non-injured wild-type and EPOR-null mice increased gradually from 25% at Day 31 to 45% at Day 35 after sham surgery. The time spent in the correct quadrant by injured mice significantly decreased at Day 34 and 35 relative to sham-operated mice (Fig. 2, $P<0.05$). No significant difference in the MWM test was observed between wild-type and EPOR-null mice after TBI.

2.4 Sensorimotor function

The incidence of forelimb footfaults during baseline (preoperatively) was approximately 4% to 5% (Fig. 3). Sham surgery alone mildly increased the frequency of footfaults at postoperative Day 1 for wild-type mice and at postoperative Days 1-14 for EPOR-null mice. TBI significantly increased the occurrence of right forelimb footfaults (contralateral to the TBI) in the wild-type mice at 1 to 21 days postinjury as compared with the non-injured wild-type mice (Fig. 3, $P<0.05$). The occurrence of right forelimb footfaults in the injured EPOR-null mice persisted over the 35-day observation time ($P<0.05$ vs. sham) and was significantly higher at 1 to 14 and 35 days post injury as compared with injured wild-type mice (Fig. 3, $P<0.05$).

Similar results were found for the hind limb contralateral to the TBI (Fig. 4). TBI significantly increased the incidence of contralateral hind limb footfaults in the wild-type mice at 1 to 7 days post-injury as compared to the non-uninjured wild-type mice ($P<0.05$) and in the EPOR-null mice at 1 to 14 days post injury as compared to the non-injured EPOR-null mice ($P<0.05$). The incidence of contralateral hind limb footfaults was significantly higher in injured EPOR-null mice than in injured wild-type mice at 4 and 7 days post injury (Fig.4, $P<0.05$).

2.5 Cell proliferation

5-bromo-2'-deoxyuridine (BrdU), an analog of thymidine, can be incorporated into the newly synthesized DNA of replicating cells during the S phase of the cell cycle. BrdU is commonly used to detect proliferating cells in living tissues (Gratzner, 1982). The number of BrdU-positive cells found in the ipsilateral DG (Figs. 5c,d) and the lesion boundary zone (Figs. 5g,h) was significantly increased in the wild-type mice and the EPOR-null mice after TBI (Fig. 5j, $P<0.05$). There was no significant difference in cell proliferation between EPOR-null and wild-type mice after TBI. BrdU-positive cells were rarely seen in the cortex (Figs. 5a,b) and DG (Figs. 5e,f) of sham animals.

2.6 Neurogenesis

Newly generated neurons were identified by double labeling for BrdU (proliferating marker) and NeuN (mature neuronal marker). Approximately 7-10% of BrdU-positive cells were NeuN/BrdU-colabeled cells in the ipsilateral DG of both EPOR-null mice and wild-type mice after TBI (Fig. 6). The percentage of NeuN/BrdU-colabeled cells was significantly higher in the lesion boundary zone in the wild-type mice than in the EPOR-null mice after TBI (Fig. 6h, $22 \pm 5\%$ vs. $4 \pm 2\%$, $P<0.05$).

2.7 Angiogenesis

von Willebrand factor (vWF)-staining has been used to identify vascular structure in the brain after TBI (Qu et al., 2005; Xiong et al., 2007). TBI alone significantly increased the density of vessels in the DG (Figs. 7c,d, $P<0.05$ vs. sham) and the cortex (Figs. 7g,h, $P<0.05$ vs. sham) of the ipsilateral hemisphere. EPOR null mice did not show significant effects on vascular density in the DG or in the cortex as compared to the wild-type mice (Fig. 7).

2.8 Accumulation of β-amyloid precursor protein and calcium

β-amyloid precursor protein (APP) staining is a universally accepted marker for detecting traumatic axonal injury (TAI) (Marmarou et al., 2005). When examined at 35 days post injury, the APP accumulation was localized in the ipsilateral thalamus in both wild-type (Figs. 8a,e) and EPOR-null mice (Figs. 8c,g). However, there were no significant differences in the thalamic APP accumulation between EPOR-null and wild-type mice after TBI. TAI was further confirmed with APP staining on free-floating sections of injured brains. The spherical (Figs. 8i,j, arrows) and segmented (Figs. 8i,j, arrows) appearance of injured axons was observed in the ipsilateral thalamus after TBI. Calcium identified with the Alizarin Red staining was found to co-accumulate with APP in the ipsilateral thalamus in the wild-type (Figs. 8b,f) and EPOR-null (Figs. 8d,h) mice after TBI. Calcium deposits were not found in any other brain areas. Calcium accumulation was more intense in the thalamus in the wild-type mice than in the EPOR-null mice after TBI ($P<0.05$).

3. Discussion

The present study has, for the first time, investigated the effect of EPOR null in the nervous system on histological and functional outcomes after TBI. The main findings of the present study are: 1) there was no significant difference in histological and functional outcomes between EPOR-null and wild-type mice in sham groups; 2) although EPOR-null mice did not exhibit greater susceptibility to TBI in terms of tissue loss in the lesion boundary zone, cell loss in the ipsilateral DG, impaired spatial learning, angiogenesis and cell proliferation, they did exhibit a significantly higher incidence of contralateral footfaults and less neurogenesis in the lesion boundary zone after TBI as compared to the wild-type mice; and 3) co-accumulation of APP and calcium was observed in the ipsilateral thalamus in both EPOR-null and wild-type mice after TBI. However, more calcium deposits were detected in wild-type mice than in EPOR-null mice after TBI.

EPORs were rescued in the endothelial cells in adult brains of the EPOR-null mice used in our present study. Adult EPOR-null mice show normal brain morphology (Chen et al., 2007). As compared to the wild-type mice, EPOR null mice did not alter the vascular density in the non-injured brains and did not affect the vascular response to TBI. Although TBI significantly increased the vascular density in the ipsilateral DG and the lesion boundary zone, there was no significant difference between both EPOR-null and wild-type mice. However, increased angiogenesis after TBI may provide neuroprotection. Exogenous EPO has been demonstrated to increase angiogenesis (Keogh et al., 2007; Li et al., 2007; Wang et al., 2004), with subsequent increased cerebral blood flow, perhaps resulting in neuroprotection (Li et al., 2007). EPOR expression is significantly up-regulated for 7 days after TBI, whereas EPO is transiently elevated (Liao et al., 2008). Taken together, our present data suggest that injury-induced increased expression of endogenous EPO/EPOR may not prevent cell loss from TBI, although higher doses of exogenous EPO (and longer duration of treatment) may be required to provide neuroprotection and promote neurorestoration after brain injury (Lu et al., 2005; Wang et al., 2004; Xiong et al., 2007; Yatsiv et al., 2005).

In the present study, cell proliferation was observed mainly in the DG and the lesion boundary zone of the ipsilateral hemisphere after TBI, without a significant difference between EPOR-null and wild-type mice. However, the percentage of BrdU/NeuN-positive cells in the lesion boundary zone was 5 times lower in the EPOR-null mice than in the wild-type mice after TBI, indicating that less cortical neurogenesis is induced in the EPOR-null mice after TBI. Neurogenesis occurs normally in the subventricular zone (SVZ) of the lateral ventricles and subgranular zone of the DG in adult mammals including humans (Kempermann et al., 2004; Zhao et al., 2008). The source of the newborn neurons in the cortex after injury is unclear. Cortical neurogenesis can be induced by degeneration (Magavi et al., 2000) or injury (Lu et

al., 2003; Xiong et al., 2007). Neural precursors isolated from damaged rat cerebral cortex after TBI have the potential to differentiate into neurons and glia (Itoh et al., 2005). However, the most likely source of newborn neurons in the lesion boundary zone is the SVZ. Stroke induces migration of newborn neuroblasts from the SVZ into the area of injury in the first 2 weeks after the insult (Arvidsson et al., 2002; Jin et al., 2003; Parent et al., 2002). Our recent work demonstrates that newly generated neurons in the SVZ migrate toward the ischemic boundary zone in rats after stroke (Zhang et al., 2004; Zhang et al., 2007). Neural precursor cells migrate toward cortical lesions from the SVZ after TBI (Goings et al., 2004; Sundholm-Peters et al., 2005). The EPOR is important for migration of regenerating neurons during post-injury recovery (Tsai et al., 2006). However, it is not clear whether there is a difference in migration of neural precursor cells from the SVZ between the EPOR-null and wild-type mice after TBI.

Spatial learning deficits in the MWM tasks have been demonstrated in rats (Lu et al., 2005; Scheff et al., 1997; Wu et al., 2008) and mice (Brody and Holtzman, 2006; Clark et al., 2007; Whalen et al., 1999; Xiong et al., 2007) in the CCI model of TBI. In the present study, cell loss in the DG region of the hippocampal formation and spatial learning deficits in the EPOR-null mice are comparable to those observed in the wild-type mice after TBI. We theorize that significant cell loss in the DG may partially contribute to impairment in spatial learning in the EPOR-null and wild-type mice after TBI. In our previous study we found that EPO significantly reduced cell loss in the DG and concomitantly improved spatial learning performance, which further supports this notion (Xiong et al., 2007).

In this study, TBI impaired sensorimotor function as revealed by the footfault test. The cortical tissue loss and related insults to connected regions after TBI likely contribute to the sensorimotor impairment. We found that EPOR-null mice with TBI showed an increased frequency of footfaults as compared to the injured wild-type mice. However, we did not find any significant difference in the lesion volume, cell proliferation, and angiogenesis in the lesion boundary zone in the EPOR-null and wild-type mice examined at day 35 after TBI, suggesting that other unknown factors, such as possible effects of more distal brain regions (Mogensen et al., 2008) and thalamic calcification (see discussions below), may contribute to the increased occurrence of footfaults in the EPOR-null mice after injury.

In the present study, calcium deposits were found only in the ipsilateral thalamus at day 35 after TBI. The functional meaning of calcium precipitation is not known. Calcium accumulation is generally believed to be detrimental to the tissues (Weber, 2004). However, thalamic calcification may have a protective role by removing excessive cytoplasmic free calcium ions, probably for the purpose of tissue repair and regeneration (Ramonet et al., 2006; Ramonet et al., 2002; Rodriguez et al., 2000). This may partially explain why EPOR-null mice with less thalamic calcification exhibited more severely impaired sensorimotor function after TBI and indicate that endogenous EPORs are essential for maintaining cellular calcium homeostasis and protecting neurons from calcium-mediated injury. Interestingly, in our present study, calcium deposits were found to co-accumulate with APP in the ipsilateral thalamus after TBI. APP accumulation indicates TAI, as revealed in the spherical and segmented appearance in Figs. 8k,l. However, there is no significant difference in APP accumulation between the EPOR-null and wild-type mice at day 35 after TBI. The relationship between APP and calcium co-accumulation in the thalamus is not clear. In TAI, massive calcium influx triggers the conversion of transport of APP from anterograde to retrograde, effectively altering local transport kinetics and developing reactive axonal swelling (Buki and Povlishock, 2006).

There are several limitations to this study. First, only young adult female mice were used in this study. Although previous data (Bruce-Keller et al., 2007; Hall et al., 2005) demonstrated that there is no significant gender difference in functional and histological outcomes in adult

mice after TBI, it is not known whether effects of brain-specific EPOR null on outcomes after TBI are gender-dependent and/or age-dependent. Some gender difference was observed in rats after TBI. For example, female rats performed significantly better than males on both motor tasks, but gender did not influence MWM performance (Wagner et al., 2004). Second, histological outcomes were examined in a single time point (i.e., Day 35 post injury) in this study. It is unclear if there is any difference in time course of histological outcomes between wild-type and EPOR-null mice after TBI.

4. Conclusions

This study demonstrates that EPOR null in the nervous system does not affect neurological function examined in adult mice under normal conditions but aggravates sensorimotor deficits, impairs cortical neurogenesis and decreases thalamic calcium accumulation after TBI, although other sites of impact injury may lead to different outcomes. Our results indicate that: 1) endogenous EPOR does not play a detectable role in the spatial learning and sensorimotor functions in adult mice under physiological conditions but plays an important role in sensorimotor functional recovery after TBI; 2) endogenous EPO/EPOR system is not essential for protecting neurons from TBI-induced cell loss although higher doses of exogenous EPO may provide neuroprotection and neurorestoration after brain injury; and 3) brain-specific EPOR may participate in post-traumatic cortical neurogenesis and thalamic calcium homeostasis.

5. Experimental procedures

5.1 Conditional rescue mice

Conditional rescue mice (C57BL6 background) were provided by Dr. Constance Tom Noguchi at NIDDK, NIH. The mouse EPOR gene was replaced by the human EPOR gene by substituting the genomic region between exon 1 to exon 8. The human EPOR gene was inactivated using a neo cassette flanked by LoxP sites inserted into intron 7. The heterozygous mice were then crossbred with transgenic mice expressing Cre recombinase under the direction of the endothelial cell specific receptor tyrosine kinase Tek (Tie2) promoter/enhancer. Expression of Cre in cells that normally express Tie2, such as embryonic endothelium, which gives rise to hematopoietic stem cells, results in recombination of the two LoxP sites and excision of the neo cassette that restores appropriately regulated expression of the EPOR gene in Cre-expressing cells and subsequent generations of cells derived from these cells. Mice from resultant litters were screened and crossed to obtain mice homozygous for the disrupted EPOR gene that carry the Tie2-Cre transgene (EPOR null) (Chen et al., 2007).

5.2 TBI model

All experimental procedures were approved by the Institutional Animal Care and Use Committee of the Henry Ford Health System.

Young adult female wild-type C57BL/6 mice (Charles River Laboratories., Inc., Wilmington, MA) and female EPOR-null mice were anesthetized intraperitoneally with 400 mg/kg body weight chloral hydrate. The body weight of mice ranged from 22 g to 25 g (4 to 5 months old). Body temperature was maintained at 37 °C by using a circulating water- heating pad. Each animal was placed in a stereotaxic frame. TBI was delivered as previously described (Xiong et al., 2007). A 4-mm diameter craniotomy was performed over the left parietal cortex adjacent to the central suture, midway between lambda and bregma. The dura was kept intact over the cortex. Injury was induced by impacting the left cortex (ipsilateral cortex) with a pneumatic piston containing a 2.5-mm-diameter tip at a rate of 4 m/second and 0.8 mm of compression. Velocity was measured with a linear velocity displacement transducer. A sham group of mice

underwent the same craniotomy but were not injured. The animals were divided into four groups: 1) sham-wild group (n=6); 2) TBI-wild group (n=8); 3) sham-null group (n=6); and 4) TBI-null group (n=10).

5.3 BrdU administration

To label proliferating cells, BrdU (100 mg/kg; Sigma, St. Louis, MO) was injected i.p. into mice daily for 10 days, starting 1 day after TBI. All animals were sacrificed at 35 days after TBI or sham.

5.4 Footfault test

To evaluate sensorimotor function, the footfault test was carried out prior to TBI and at 1, 4, 7, 14, 21, 28, and 35 days after TBI or sham by an investigator blind to the individual groups. The mice were allowed to walk on a grid (12 cm × 57 cm with 1.3 cm × 1.3 cm diameter openings). With each weight-bearing step, a paw might fall or slip between the wires and, if this occurred, it was recorded as a footfault. A total of 50 steps were recorded for each right forelimb and hind limb (Baskin et al., 2003; Xiong et al., 2007).

5.5 Morris water maze test

To detect spatial learning deficits, a recent version of the MWM test was used (Choi et al., 2006; Lu et al., 2005; Xiong et al., 2007). All animals were tested during the last five days (i.e., from 31-35 days after TBI or sham operation) before sacrifice. Data collection was automated by the HVS Image 2020 Plus Tracking System (US HVS Image, San Diego, CA.). For data collection, a white pool (1.2 m in diameter) was subdivided into four equal quadrants formed by imaging lines. At the start of a trial, the mouse was placed randomly at one of four fixed starting points, facing toward the wall (designated North, South, East and West) and allowed to swim for 90 seconds or until they found the platform within 90 seconds. If the animal found the platform, it was allowed to remain on it for 10 seconds. If the animal failed to find the platform within 90 seconds, it was placed on the platform for 10 seconds. Throughout the test period the platform was located in the NE quadrant 1 cm below water in a randomly changing position, including locations against the wall, toward the middle of the pool or off-center, but always within the target quadrant. If the animal was unable to find the platform within 90 seconds, the trial was terminated and a maximum score of 90 seconds was assigned. If the animal reached the platform within 90 seconds, the percentage of time traveled within the NE (correct) quadrant was calculated relative to the total amount of time spent swimming before reaching the platform and employed for statistical analysis. The advantage of this version of the water maze is that each trial or set of trials takes on the key characteristics of a probe trial because the platform is not in a fixed location within the target quadrant (Choi et al., 2006).

5.6 Tissue preparation and measurement of lesion volume

At 35 days after TBI, mice were anesthetized intraperitoneally with chloral hydrate, and perfused transcardially first with saline solution, followed by 4% paraformaldehyde in 0.1 M phosphate buffered saline (PBS), pH 7.4. The brains were removed and post-fixed in 4% paraformaldehyde at room temperature for 48 h. The brain tissue was cut into 7 equally spaced (1 mm) coronal blocks, and processed for paraffin sectioning. A series of adjacent 6-μm thick sections were cut from each block in the coronal plane and stained with hematoxylin and eosin (H&E). To measure lesion volume the 7 brain sections were traced by a microcomputer imaging device (MCID) (Imaging Research, St. Catharine's, Ontario, Canada), as previously described (Chen et al., 2005; Xiong et al., 2007). The indirect lesion area was calculated (i.e., the intact area of the ipsilateral hemisphere is subtracted from the area of the contralateral hemisphere) (Chen et al., 2005), and the lesion volume presented as a volume percentage of the lesion

compared with the contralateral hemisphere. H&E sections from blocks E and F containing hippocampus were used to acquire images of the DG at 20x magnification.

5.7 Immunohistochemistry

To examine cell proliferation, coronal sections were immunostained with mouse anti-BrdU (Xiong et al., 2007). Coronal sections were deparaffinized and rehydrated. Antigen retrieval was performed by boiling sections in 10 mM citrate buffer (pH 6.0) for 10 min. After washing with PBS, sections were incubated with 0.3% H_2O_2 in PBS for 10 min, blocked with 1% BSA containing 0.3% Triton-X 100 at room temperature for 1 h, and incubated with mouse anti-BrdU (1:200; Dako, Carpinteria, CA) at 4 °C overnight. After washing, sections were incubated with biotinylated anti-mouse antibody (1:200; Vector Laboratories, Inc., Burlingame, CA) at room temperature for 30 min. After washing, sections were incubated with an avidin-biotin-peroxidase system (ABC kit, Vector Laboratories, Inc., Burlingame, CA). Diaminobenzidine (Sigma, St. Louis, MO) was then used as a chromogen. Sections were counterstained with hematoxylin.

To identify vascular structure, coronal sections were immunohistochemically stained with von Willebrand factor (vWF) antibody (Xiong et al., 2007). Brain sections were deparaffinized and then incubated with 0.4% Pepsin solution at 37 °C for 1 h. After washing, the sections were blocked with 1% BSA at room temperature for 1 h, and then incubated with rabbit anti-human vWF (1:200; DakoCytomation, Carpinteria, CA) at 4 °C overnight. After washing, sections were incubated with biotinylated anti-rabbit antibody (1:200; Vector Laboratories, Inc., Burlingame, CA) and then with an avidin-biotin-peroxidase system, visualized with diaminobenzidine and counterstained with hematoxylin as described above.

BrdU-positive cells and vWF-stained vascular structures in the ipsilateral DG and lesion boundary zone were examined at 20x magnification and counted. The cells with BrdU (brown stained) that clearly localized to the nucleus (hematoxylin stained) were counted as BrdU-positive cells.

To detect axonal injury, following deparaffinization, antigen retrieval and blocking described above for BrdU staining, coronal sections were immunohistochemically stained with mouse anti-amyloid precursor protein (MAB348, 1:400; Chemicon Int., Temecula, CA) at 4 °C overnight. After washing, sections were incubated with biotinylated anti-mouse antibody (1:200; Vector Laboratories, Inc., Burlingame, CA), and then with an avidin-biotin-peroxidase system, visualized with diaminobenzidine and counterstained with hematoxylin, as described above.

In addition, calcium deposits in the coronal sections were detected with the Alizarin Red standard staining in adjacent coronal sections (Kato et al., 1995). The percentage of APP or calcium accumulation in the thalamus is presented as a proportional area (staining area divided by tissue areas).

5.8 Immunofluorescent staining

Newly generated neurons were identified by double labeling for BrdU and NeuN. After dehydration, tissue sections were boiled in 10 mM citric acid buffer (pH 6) for 10 min. After washing with PBS, sections were incubated in 2.4 N HCl at 37 °C for 20 min. Sections were incubated with 1% BSA containing 0.3% Triton-X-100 in PBS. Sections were then incubated with mouse anti-NeuN antibody (1:200; Chemicon, Temecula, CA) at 4 °C overnight. FITC-conjugated anti-mouse antibody (1:400; Jackson ImmunoResearch, West Grove, PA) was added to sections at room temperature for 2 h. Sections were then incubated with mouse anti-BrdU antibody (1:200; Dako, Glostrup, Denmark) at 4 °C overnight. Sections were then

incubated with Cy3-conjugated anti-mouse or anti-rabbit antibody (1:400; Jackson ImmunoResearch, West Grove, PA) at room temperature for 2 h. Each of the steps was followed by three 5-min rinses in PBS. Tissue sections were mounted with Vectashield mounting medium (Vector laboratories, Burlingame, CA).

5.9 Cell counting and quantization

Cell counts were performed by observers blinded to the individual status of the animals. Five sections cut from the dorsal DG in 100-μm intervals were analyzed with a microscope (Nikon i80) at 400x magnification via the MCID system. All counting was performed on a computer monitor to improve visualization and in one focal plane to avoid oversampling (Zhang et al., 2002). To evaluate whether EPOR null in the brain would affect neuronal damage after TBI, the number of cells was counted in the DG using the MCID system. Counts were averaged and normalized by measuring the linear distance (in mm) of the DG for each section. This method permits a meaningful comparison of differences between groups. To determine cell proliferation, the MCID system was used to count the total number of BrdU-positive cells in the lesion boundary zone and the DG regions of the hippocampus. The number of BrdU-positive cells was expressed in cells/mm^2. To evaluate neurogenesis in the DG and the cortex, additional sections were used by calculating the density of BrdU-labeled cells and BrdU/NeuN-colabeled cells (Xiong et al., 2007; Zhang et al., 2002). The number of BrdU-positive cells (red stained) and NeuN/BrdU-colabeled cells (yellow after merge) were counted in the DG and the lesion boundary zone. The percentage of NeuN/BrdU-colabeled cells over the total number of BrdU-positive cells in the corresponding regions (DG or cortex) was estimated and used as a parameter for neurogenesis.

5.10 Statistical Analyses

All data are presented as the means with standard deviations (SD). For lesion volume, cell counting, APP and calcium accumulation, and vWF-stained vascular density, a one-way analysis of variance (ANOVA) followed by post hoc Student-Newman-Keuls (SNK) tests was used to compare the difference between different groups. Data were analyzed by ANOVA for repeated measurements of functional tests (spatial performance and sensorimotor function). Statistical significance was set at $P<0.05$.

Acknowledgements

This work was supported by NINDS grants RO1 NS52280, PO1 NS42345 and NIDDK Intramural Research.

References

Arvidsson A, Collin T, Kirik D, Kokaia Z, Lindvall O. Neuronal replacement from endogenous precursors in the adult brain after stroke. Nat Med 2002;8:963–970. [PubMed: 12161747]

Baskin YK, Dietrich WD, Green EJ. Two effective behavioral tasks for evaluating sensorimotor dysfunction following traumatic brain injury in mice. J Neurosci Methods 2003;129:87–93. [PubMed: 12951236]

Brines ML, Ghezzi P, Keenan S, Agnello D, de Lanerolle NC, Cerami C, Itri LM, Cerami A. Erythropoietin crosses the blood-brain barrier to protect against experimental brain injury. Proc Natl Acad Sci U S A 2000;97:10526–10531. [PubMed: 10984541]

Brody DL, Holtzman DM. Morris water maze search strategy analysis in PDAPP mice before and after experimental traumatic brain injury. Exp Neurol 2006;197:330–340. [PubMed: 16309676]

Bruce-Keller AJ, Dimayuga FO, Reed JL, Wang C, Angers R, Wilson ME, Dimayuga VM, Scheff SW. Gender and estrogen manipulation do not affect traumatic brain injury in mice. J Neurotrauma 2007;24:203–215. [PubMed: 17263684]

Buki A, Povlishock JT. All roads lead to disconnection?--Traumatic axonal injury revisited. Acta Neurochir (Wien) 2006;148:181–193. [PubMed: 16362181]discussion 193-184

Chen J, Zhang C, Jiang H, Li Y, Zhang L, Robin A, Katakowski M, Lu M, Chopp M. Atorvastatin induction of VEGF and BDNF promotes brain plasticity after stroke in mice. J Cereb Blood Flow Metab 2005;25:281–290. [PubMed: 15678129]

Chen ZY, Asavaritikrai P, Prchal JT, Noguchi CT. Endogenous erythropoietin signaling is required for normal neural progenitor cell proliferation. J Biol Chem 2007;282:25875–25883. [PubMed: 17604282]

Cherian L, Goodman JC, Robertson C. Neuroprotection with erythropoietin administration following controlled cortical impact injury in rats. J Pharmacol Exp Ther 2007;322:789–794. [PubMed: 17470644]

Choi SH, Woodlee MT, Hong JJ, Schallert T. A simple modification of the water maze test to enhance daily detection of spatial memory in rats and mice. J Neurosci Methods 2006;156:182–193. [PubMed: 16621016]

Clark RS, Vagni VA, Nathaniel PD, Jenkins LW, Dixon CE, Szabo C. Local administration of the poly (ADP-ribose) polymerase inhibitor INO-1001 prevents NAD+ depletion and improves water maze performance after traumatic brain injury in mice. J Neurotrauma 2007;24:1399–1405. [PubMed: 17711401]

Fox GB, Faden AI. Traumatic brain injury causes delayed motor and cognitive impairment in a mutant mouse strain known to exhibit delayed Wallerian degeneration. J Neurosci Res 1998;53:718–727. [PubMed: 9753199]

Goings GE, Sahni V, Szele FG. Migration patterns of subventricular zone cells in adult mice change after cerebral cortex injury. Brain Res 2004;996:213–226. [PubMed: 14697499]

Grasso G, Sfacteria A, Meli F, Fodale V, Buemi M, Iacopino DG. Neuroprotection by erythropoietin administration after experimental traumatic brain injury. Brain Res 2007;1182:99–105. [PubMed: 17935704]

Gratzner HG. Monoclonal antibody to 5-bromo- and 5-iododeoxyuridine: A new reagent for detection of DNA replication. Science 1982;218:474–475. [PubMed: 7123245]

Hall ED, Bryant YD, Cho W, Sullivan PG. Evolution of post-traumatic neurodegeneration after controlled cortical impact traumatic brain injury in mice and rats as assessed by the de olmos silver and fluorojade staining methods. J Neurotrauma 2008;25:235–247. [PubMed: 18352837]

Hall ED, Gibson TR, Pavel KM. Lack of a gender difference in post-traumatic neurodegeneration in the mouse controlled cortical impact injury model. J Neurotrauma 2005;22:669–679. [PubMed: 15941376]

Itoh T, Satou T, Hashimoto S, Ito H. Isolation of neural stem cells from damaged rat cerebral cortex after traumatic brain injury. Neuroreport 2005;16:1687–1691. [PubMed: 16189478]

Jin G, Omori N, Li F, Nagano I, Manabe Y, Shoji M, Abe K. Protection against ischemic brain damage by GDNF affecting cell survival and death signals. Neurol Res 2003;25:249–253. [PubMed: 12739232]

Kato H, Araki T, Itoyama Y, Kogure K. Calcium deposits in the thalamus following repeated cerebral ischemia and long-term survival in the gerbil. Brain Res Bull 1995;38:25–30. [PubMed: 7552371]

Kempermann G, Wiskott L, Gage FH. Functional significance of adult neurogenesis. Curr Opin Neurobiol 2004;14:186–191. [PubMed: 15082323]

Keogh CL, Yu SP, Wei L. The effect of recombinant human erythropoietin on neurovasculature repair after focal ischemic stroke in neonatal rats. J Pharmacol Exp Ther 2007;322:521–528. [PubMed: 17494864]

Li Y, Lu Z, Keogh CL, Yu SP, Wei L. Erythropoietin-induced neurovascular protection, angiogenesis, and cerebral blood flow restoration after focal ischemia in mice. J Cereb Blood Flow Metab 2007;27:1043–1054. [PubMed: 17077815]

Liao ZB, Zhi XG, Shi QH, He ZH. Recombinant human erythropoietin administration protects cortical neurons from traumatic brain injury in rats. Eur J Neurol 2008;15:140–149. [PubMed: 18093155]

Lu D, Mahmood A, Qu C, Goussev A, Schallert T, Chopp M. Erythropoietin enhances neurogenesis and restores spatial memory in rats after traumatic brain injury. J Neurotrauma 2005;22:1011–1017. [PubMed: 16156716]

Lu D, Mahmood A, Zhang R, Copp M. Upregulation of neurogenesis and reduction in functional deficits following administration of DEtA/NONOate, a nitric oxide donor, after traumatic brain injury in rats. J Neurosurg 2003;99:351–361. [PubMed: 12924710]

Magavi SS, Leavitt BR, Macklis JD. Induction of neurogenesis in the neocortex of adult mice. Nature 2000;405:951–955. [PubMed: 10879536]

Marmarou CR, Walker SA, Davis CL, Povlishock JT. Quantitative analysis of the relationship between intra- axonal neurofilament compaction and impaired axonal transport following diffuse traumatic brain injury. J Neurotrauma 2005;22:1066–1080. [PubMed: 16238484]

Mogensen J, Jensen C, Kingod SC, Hansen A, Larsen JA, Mala H. Erythropoietin improves spatial delayed alternation in a T-maze in fimbria-fornix transected rats. Behav Brain Res 2008;186:215–221. [PubMed: 17888525]

Parent JM, Vexler ZS, Gong C, Derugin N, Ferriero DM. Rat forebrain neurogenesis and striatal neuron replacement after focal stroke. Ann Neurol 2002;52:802–813. [PubMed: 12447935]

Qu C, Lu D, Goussev A, Schallert T, Mahmood A, Chopp M. Effect of atorvastatin on spatial memory, neuronal survival, and vascular density in female rats after traumatic brain injury. J Neurosurg 2005;103:695–701. [PubMed: 16266052]

Ramonet D, de Yebra L, Fredriksson K, Bernal F, Ribalta T, Mahy N. Similar calcification process in acute and chronic human brain pathologies. J Neurosci Res 2006;83:147–156. [PubMed: 16323208]

Ramonet D, Pugliese M, Rodriguez MJ, de Yebra L, Andrade C, Adroer R, Ribalta T, Mascort J, Mahy N. Calcium precipitation in acute and chronic brain diseases. J Physiol Paris 2002;96:307–312. [PubMed: 12445910]

Rodriguez MJ, Bernal F, Andres N, Malpesa Y, Mahy N. Excitatory amino acids and neurodegeneration: a hypothetical role of calcium precipitation. Int J Dev Neurosci 2000;18:299–307. [PubMed: 10715584]

Sakanaka M, Wen TC, Matsuda S, Masuda S, Morishita E, Nagao M, Sasaki R. In vivo evidence that erythropoietin protects neurons from ischemic damage. Proc Natl Acad Sci U S A 1998;95:4635–4640. [PubMed: 9539790]

Scheff SW, Baldwin SA, Brown RW, Kraemer PJ. Morris water maze deficits in rats following traumatic brain injury: lateral controlled cortical impact. J Neurotrauma 1997;14:615–627. [PubMed: 9337124]

Smith DH, Soares HD, Pierce JS, Perlman KG, Saatman KE, Meaney DF, Dixon CE, McIntosh TK. A model of parasagittal controlled cortical impact in the mouse: cognitive and histopathologic effects. J Neurotrauma 1995;12:169–178. [PubMed: 7629863]

Sundholm-Peters NL, Yang HK, Goings GE, Walker AS, Szele FG. Subventricular zone neuroblasts emigrate toward cortical lesions. J Neuropathol Exp Neurol 2005;64:1089–1100. [PubMed: 16319719]

Tsai PT, Ohab JJ, Kertesz N, Groszer M, Matter C, Gao J, Liu X, Wu H, Carmichael ST. A critical role of erythropoietin receptor in neurogenesis and post-stroke recovery. J Neurosci 2006;26:1269–1274. [PubMed: 16436614]

Verdonck O, Lahrech H, Francony G, Carle O, Farion R, Van de Looij Y, Remy C, Segebarth C, Payen JF. Erythropoietin protects from post-traumatic edema in the rat brain. J Cereb Blood Flow Metab 2007;27:1369–1376. [PubMed: 17264861]

Wagner AK, Willard LA, Kline AE, Wenger MK, Bolinger BD, Ren D, Zafonte RD, Dixon CE. Evaluation of estrous cycle stage and gender on behavioral outcome after experimental traumatic brain injury. Brain Res 2004;998:113–121. [PubMed: 14725974]

Wang L, Zhang Z, Wang Y, Zhang R, Chopp M. Treatment of stroke with erythropoietin enhances neurogenesis and angiogenesis and improves neurological function in rats. Stroke 2004;35:1732–1737. [PubMed: 15178821]

Weber JT. Calcium homeostasis following traumatic neuronal injury. Curr Neurovasc Res 2004;1:151–171. [PubMed: 16185191]

Whalen MJ, Carlos TM, Dixon CE, Schiding JK, Clark RS, Baum E, Yan HQ, Marion DW, Kochanek PM. Effect of traumatic brain injury in mice deficient in intercellular adhesion molecule-1: assessment of histopathologic and functional outcome. J Neurotrauma 1999;16:299–309. [PubMed: 10225216]

Wu H, Lu D, Jiang H, Xiong Y, Qu C, Li B, Mahmood A, Zhou D, Chopp M. Simvastatin-mediated upregulation of VEGF and BDNF, activation of the PI3K/Akt pathway, and increase of neurogenesis are associated with therapeutic improvement after traumatic brain injury. J Neurotrauma 2008;25:130–139. [PubMed: 18260796]

Xiong Y, Mahmood A, Lu D, Qu C, Goussev A, Schallert T, Chopp M. Role of gender in outcome after traumatic brain injury and therapeutic effect of erythropoietin in mice. Brain Res 2007;1185:301–312. [PubMed: 17976541]

Xiong Y, Shie FS, Zhang J, Lee CP, Ho YS. Prevention of mitochondrial dysfunction in post-traumatic mouse brain by superoxide dismutase. J Neurochem 2005;95:732–744. [PubMed: 16248885]

Yatsiv I, Grigoriadis N, Simeonidou C, Stahel PF, Schmidt OI, Alexandrovitch AG, Tsenter J, Shohami E. Erythropoietin is neuroprotective, improves functional recovery, and reduces neuronal apoptosis and inflammation in a rodent model of experimental closed head injury. Faseb J 2005;19:1701–1703. [PubMed: 16099948]

Zhang J, Li Y, Cui Y, Chen J, Lu M, Elias SB, Chopp M. Erythropoietin treatment improves neurological functional recovery in EAE mice. Brain Res 2005;1034:34–39. [PubMed: 15713257]

Zhang R, Wang Y, Zhang L, Zhang Z, Tsang W, Lu M, Zhang L, Chopp M. Sildenafil (Viagra) induces neurogenesis and promotes functional recovery after stroke in rats. Stroke 2002;33:2675–2680. [PubMed: 12411660]

Zhang R, Zhang Z, Wang L, Wang Y, Gousev A, Zhang L, Ho KL, Morshead C, Chopp M. Activated neural stem cells contribute to stroke-induced neurogenesis and neuroblast migration toward the infarct boundary in adult rats. J Cereb Blood Flow Metab 2004;24:441–448. [PubMed: 15087713]

Zhang RL, LeTourneau Y, Gregg SR, Wang Y, Toh Y, Robin AM, Zhang ZG, Chopp M. Neuroblast division during migration toward the ischemic striatum: a study of dynamic migratory and proliferative characteristics of neuroblasts from the subventricular zone. J Neurosci 2007;27:3157–3162. [PubMed: 17376977]

Zhao C, Deng W, Gage FH. Mechanisms and functional implications of adult neurogenesis. Cell 2008;132:645–660. [PubMed: 18295581]

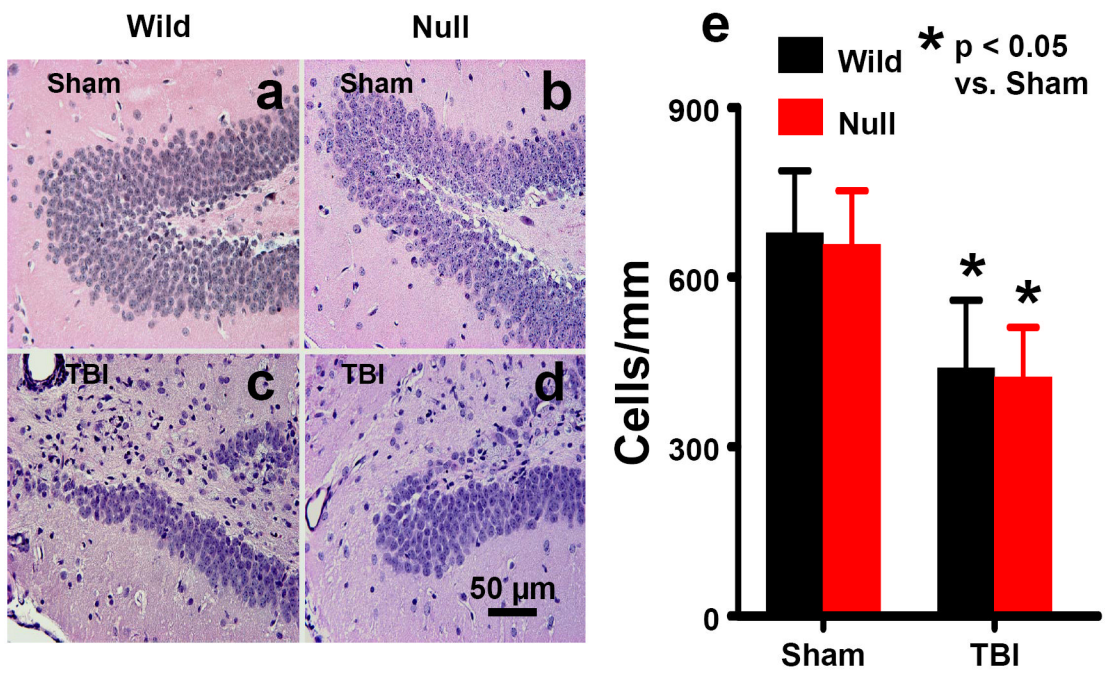

Fig. 1.

Cell density in the DG examined at 35 days after TBI or sham. H&E staining: a-d. TBI caused significant cell loss in the ipsilateral DG (mainly in the dorsal blade) in the wild-type (c) and EPOR-null mice (d). Scale bar: 50μm (a-d). The cell number in the DG is shown in (e). Data represent mean with SD. N (mice/group) = 6 (Sham-Wild); 8 (TBI-Wild); 6 (Sham-Null); 10 (TBI-Null).

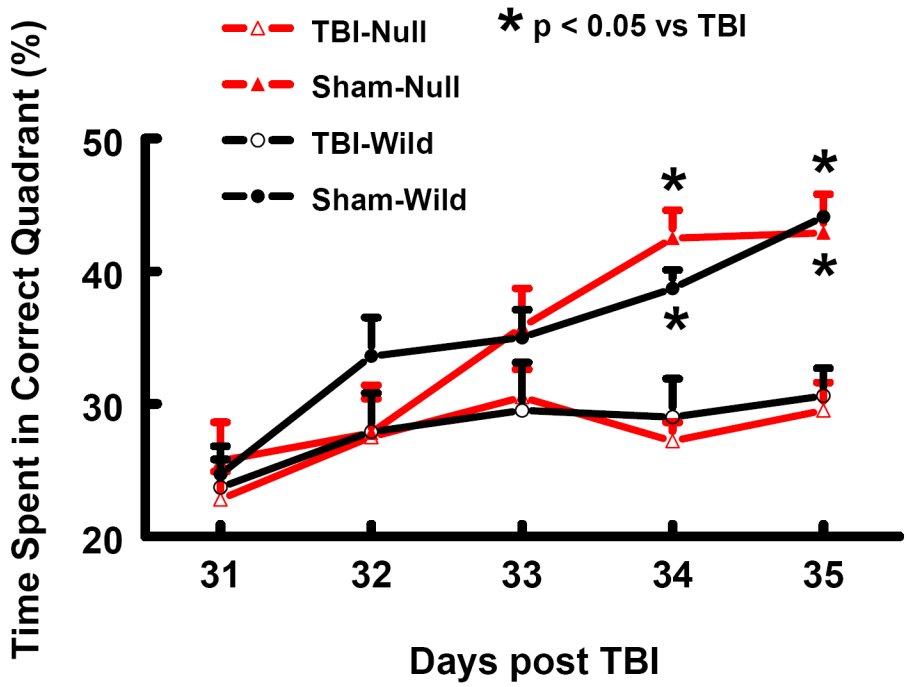

Fig. 2.

Spatial learning function examined at 31-35 days after TBI or sham. TBI significantly impaired spatial learning performance (time spent in the correct quadrant) at 34 and 35 days after TBI measured by a recent version of the water maze test. Data represent mean with SD. N (mice/group) = 6 (Sham-Wild); 8 (TBI-Wild); 6 (Sham-Null); 10 (TBI-Null).

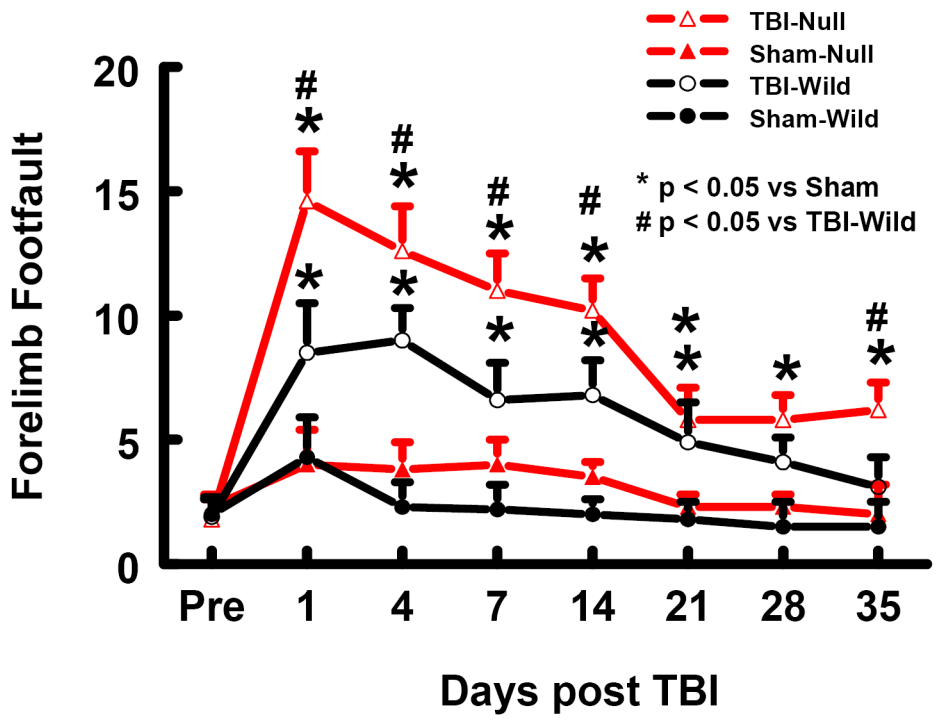

Fig. 3.

Sensorimotor function (forelimb footfault) before and after TBI or sham. “Pre” represents pre-injury level. TBI impaired sensorimotor performance (contralateral forelimb footfault). Data represent mean with SD. N (mice/group) = 6 (Sham-Wild); 8 (TBI-Wild); 6 (Sham-Null); 10 (TBI-Null).

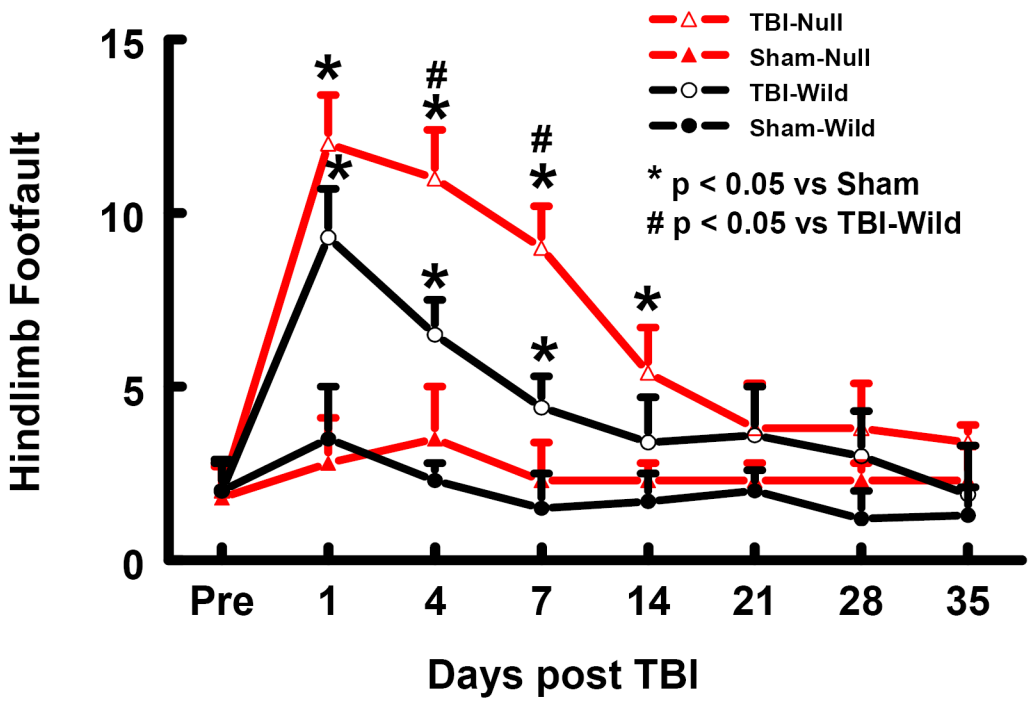

Fig. 4.

Sensorimotor function (hind limb footfault) before and after TBI or sham. “Pre” represents pre-injury level. TBI impaired sensorimotor performance (contralateral hind limb footfault). Data represent mean with SD. N (mice/group) = 6 (Sham-Wild); 8 (TBI-Wild); 6 (Sham-Null); 10 (TBI-Null).

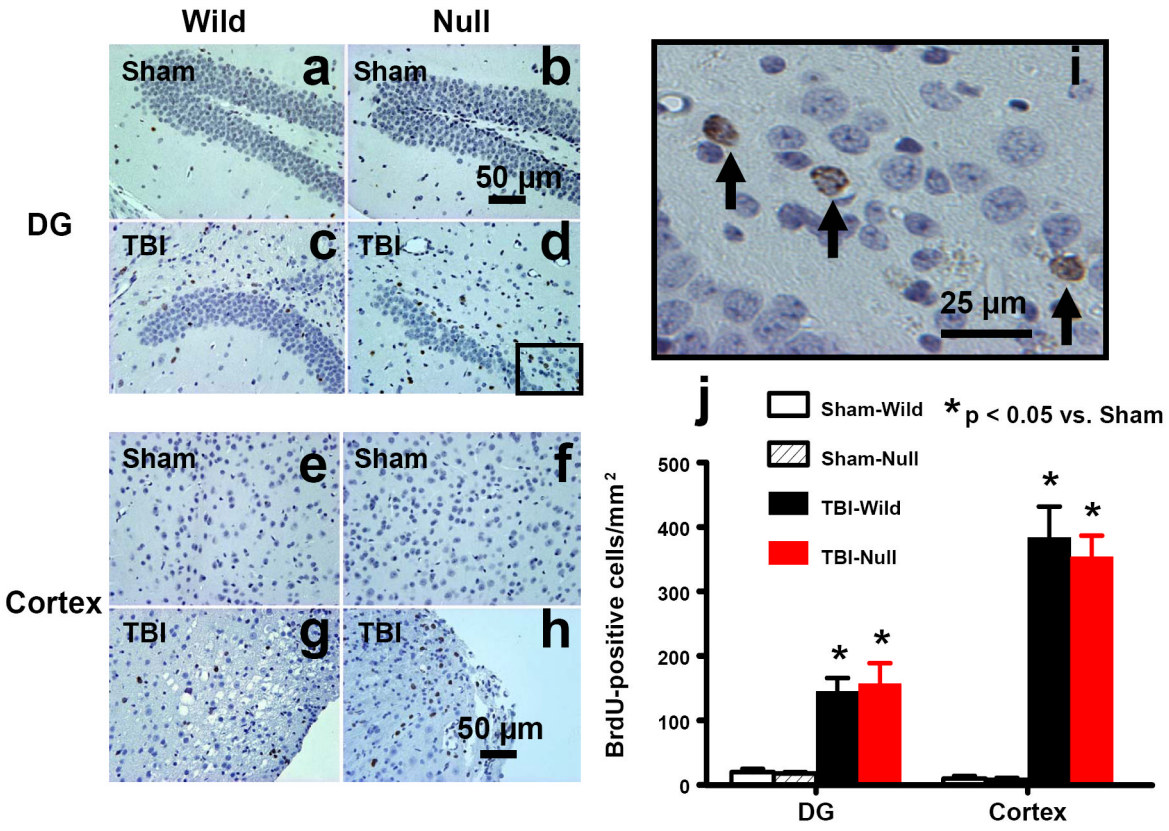

Fig. 5.

Cell proliferation in the ipsilateral DG and cortex 35 days after TBI or sham. TBI significantly increased the number of BrdU-positive cells in the ipsilateral DG (c and d) and cortex (g and h). The cells with BrdU (brown stained) that clearly localize to the nucleus (hematoxylin stained) are counted as BrdU-positive cells (i, arrows). Scale bars: 50μm (a-h); 25μm (i). The number of BrdU-positive cells is shown in (j). Data represent mean with SD. N (mice/group) = 6 (Sham-Wild); 8 (TBI-Wild); 6 (Sham-Null); 10 (TBI-Null).

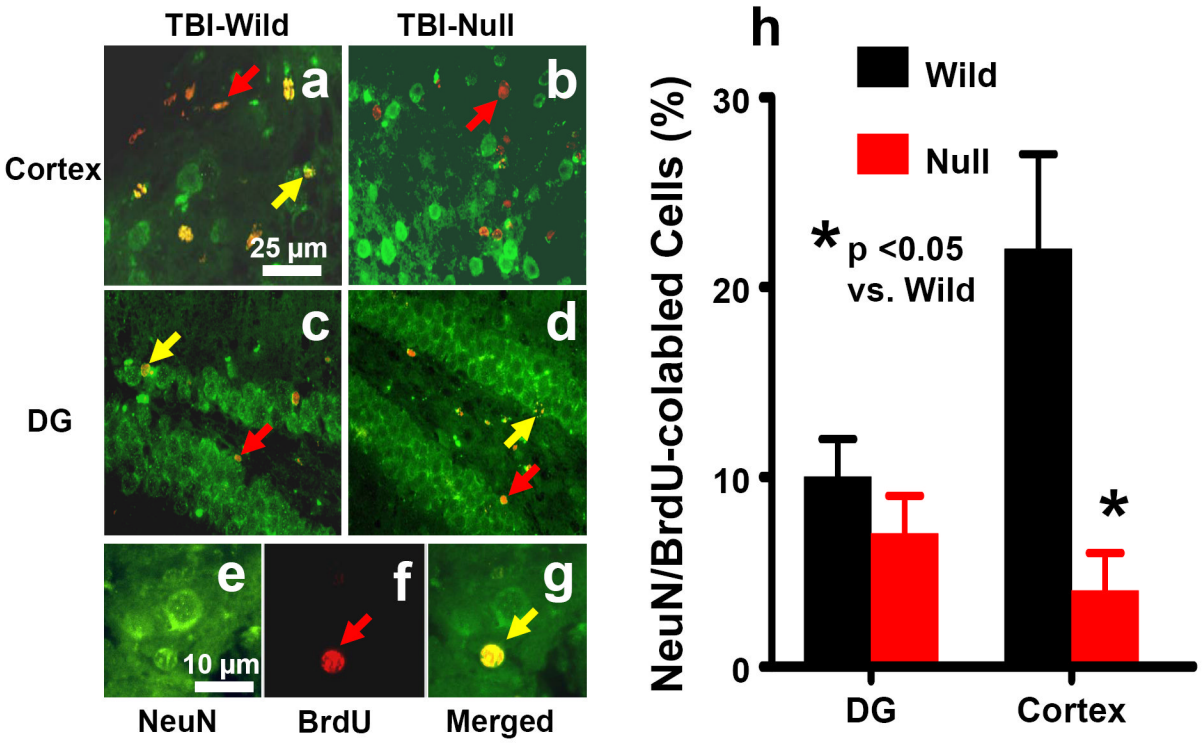

Fig. 6.

Double fluorescent staining for BrdU (red) and NeuN (green) to identify neurogenesis (yellow after merge) in the cortex (a and b, arrow as example) and the dentate gyrus (c and d, arrow as example) of the ipsilateral, injured hemisphere at 35 days after TBI. Newborn BrdU-positive cells (red, f) differentiate into neurons expressing NeuN (yellow, g). Scale bars: 25μm (a-d); 10μm (e-g). The percentage of NeuN/BrdU-colabeled cells is shown in (h). Data represent mean with SD. N (mice/group) = 6 (Sham-Wild); 8 (TBI-Wild); 6 (Sham-Null); 10 (TBI-Null).

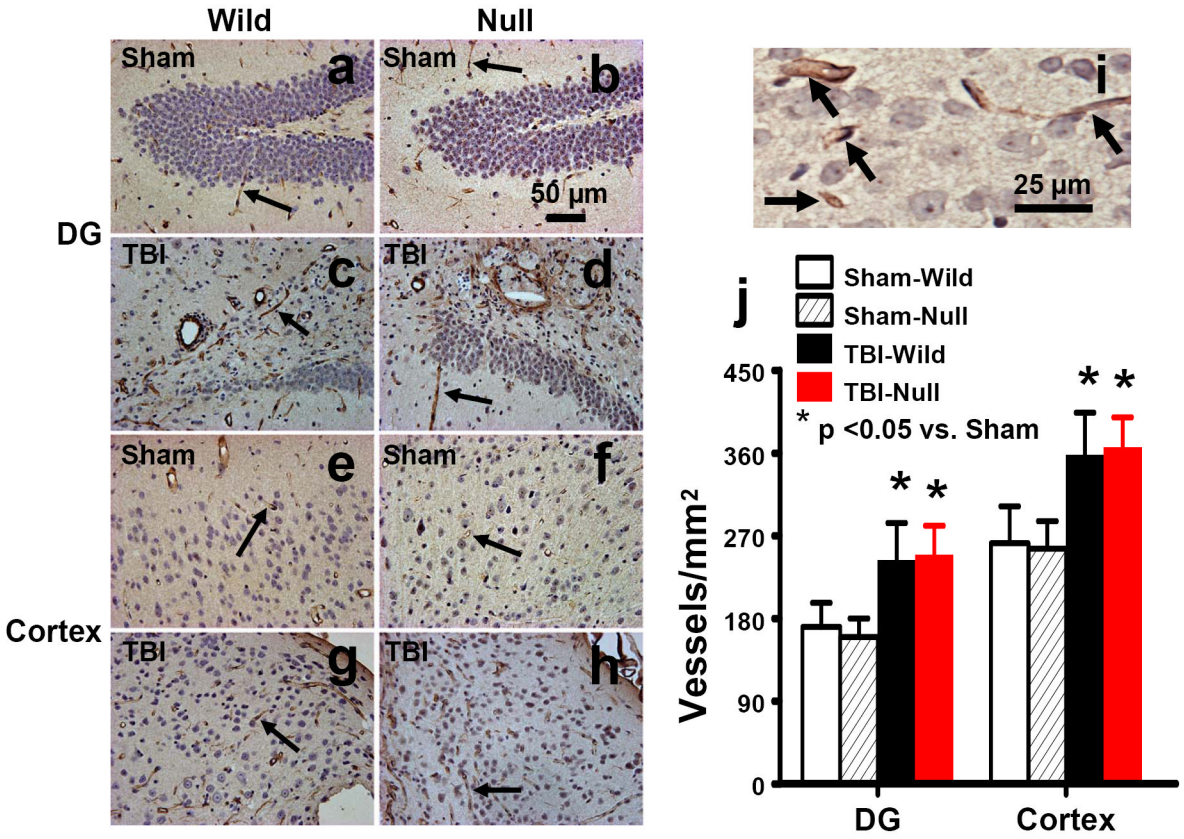

Fig. 7.

vWF staining for vascular structure in the ipsilateral DG and cortex at 35 days after TBI or sham. TBI significantly increased the density of vasculature in the ipsilateral DG (c and d) and cortex (g and h). The vasculature with vWF staining is counted (brown stained) as shown in (i, arrows). Scale bars: 50μm (a-h); 25μm (i). The density of vWF-stained vasculature is shown in (j). Data represent mean with SD. N (mice/group) = 6 (Sham-Wild); 8 (TBI-Wild); 6 (Sham-Null); 10 (TBI-Null).

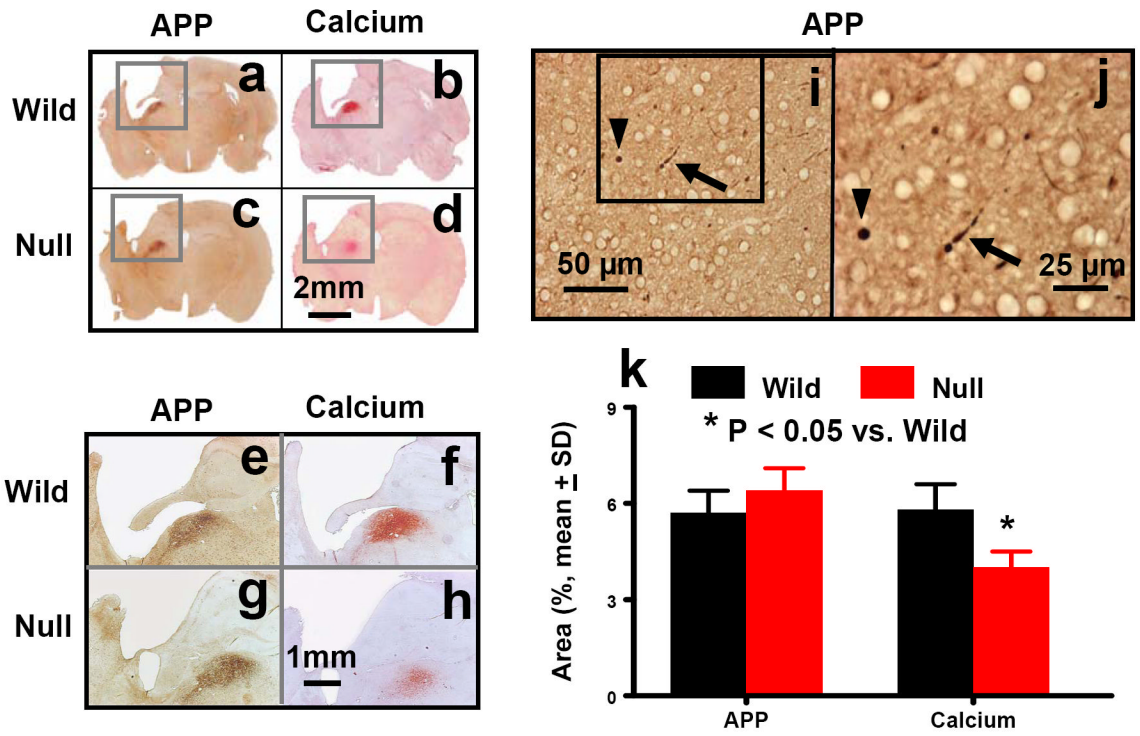

Fig. 8.

APP and calcium staining in the ipsilateral DG and cortex at 35 days after TBI. APP accumulated in the ipsilateral thalamus in both wild-type (a, e, i, and j) and EPOR-null (c and g) mice after TBI. Traumatic axonal injury was confirmed with APP staining on free floating sections (50 μm) of injured brains. The spherical (i and j, arrowheads) and segmented (i and j, arrows) appearance of injured axons was observed in the ipsilateral thalamus after TBI. Calcium deposits stained with Arilazan Red were found in the ipsilateral thalamus in both wild-type (b, f, and j) and EPOR-null mice (d and h) after TBI. Note an overlap of APP with calcium staining in adjacent sections. Scale bars: 2 mm (a-d); 1 mm (e-h); 50 μm (i); and 25 μm (j). The percentage of area of APP and calcium deposits is shown in (k). Data represent mean with SD. N (mice/group) = 6 (Sham-Wild); 8 (TBI-Wild); 6 (Sham-Null); 10 (TBI-Null).